

LA-UR-21-31485

Approved for public release; distribution is unlimited.

Title: 17-7PH Housing Weld Report FY21

Author(s): Hawk, Cheryl Lynn
Glover, Alexandra Gannon
Mier, Ryan Miguel
McKamey, Michaela Anne
Wiest, Stephen P.
Bloom, Rose Anne
Winter, William Paul III
Black, Amber Nalani
Duffield, Andrew Nathan
Gibbs, Paul Jacob

Intended for: Report

Issued: 2021-11-18

Disclaimer:

Los Alamos National Laboratory, an affirmative action/equal opportunity employer, is operated by Triad National Security, LLC for the National Nuclear Security Administration of U.S. Department of Energy under contract 89233218CNA000001. By approving this article, the publisher recognizes that the U.S. Government retains nonexclusive, royalty-free license to publish or reproduce the published form of this contribution, or to allow others to do so, for U.S. Government purposes. Los Alamos National Laboratory requests that the publisher identify this article as work performed under the auspices of the U.S. Department of Energy. Los Alamos National Laboratory strongly supports academic freedom and a researcher's right to publish; as an institution, however, the Laboratory does not endorse the viewpoint of a publication or guarantee its technical correctness.

17-7PH Housing Weld Report FY21

By

Cheryl L. Hawk, Allie G. Glover, Ryan M. Mier, Michaela A. McKamey, Stephen P. Wiest, Rose A. Bloom, Will P. Winter, Amber N. Black, Andrew N. Duffield, and Paul J. Gibbs.

Los Alamos National Laboratory

11/18/2021

Executive Summary

This report presents the work performed for welding 17-7PH stainless steel hemispheres, flanges, and accelerometer blocks. This includes weld development, microhardness measurements, calculated strengths, and distortion measurements after welding and heat treatment. The results of this report are utilized to propose a recommended welding procedure which was implemented for this experiment.

1.0 Introduction

This weld report summarizes the work performed for the 17-7PH Project, the reasoning behind the tasks performed, and the results that influenced final manufacturing.

2.0 Background

17-7PH stainless steel is a semi-austenitic, precipitation-hardened stainless steel which exhibits high strength and moderate ductility in the 1050TH heat treatment condition, in combination with moderate corrosion resistance. The composition of 17-7PH stainless steel is shown in Table 1. Typically, 17-7PH is fabricated (formed, welded, and machined) in the austenitic condition which exhibits moderate strength and high ductility.

The heat treatment of 17-7PH stainless steel consists of three steps. First, an annealing heat treatment at a temperature within the single phase austenitic region ensures all alloying elements are in solution. Typically a temperature of 1066 °C is recommended for a time of 90 min. This results in an austenitic microstructure retained upon quenching to room temperature and is termed the mill anneal (A) condition. Following the application of the mill anneal heat treatment, fabrication (forming, welding, machining, etc.) usually takes place due to the reduced strength and increased elongation associated with the fully austenitic microstructure. Following fabrication, a second heat treatment, called austenite conditioning (T-condition), is applied at a temperature of 760 °C for 90 minutes during which carbide precipitation occurs. Upon quenching from the austenite conditioning heat treatment, austenite is expected to transform entirely to BCC/BCT martensite. Finally, an aging heat treatment is applied at a temperature of 566 °C for 90 minutes resulting the in the precipitation of NiAl precipitates. Following aging, the 17-7PH stainless steel is considered to be in the TH 1050 heat treatment condition.

Table 1: composition of 17-7 PH stainless steel [ref].

C	Mn	Si	Cr	Ni	Al	Fe
0.09	1.00	1.00	16.00 – 18.00	6.50 – 7.75	0.75 – 1.50	Bal.

3.0 Objective

The goal of this work was two-fold: (1) to create a hermetic seal between a hemisphere (hemi) and a flange and (2) securely attach accelerometer blocks to the poles of the hemis. The requirements for welding the flange were as follows:

- Penetration Depth: weld must exceed the thickness of the hemi
- Minimize Distortion: flanges must form a hermetic seal when hemis are joined
- Hermetic Seal: weld must form a hermetic seal between the flange and hemi
- Weld Strength: must be a minimum of 50% of the base material strength

The requirements for the accelerometer blocks were as follows:

- Minimize Distortion: hemi must maintain internal dimensions

Eight hemis were welded resulting in four complete sets of spheres. A schematic of a hemi to be welded is shown in Figure 1.

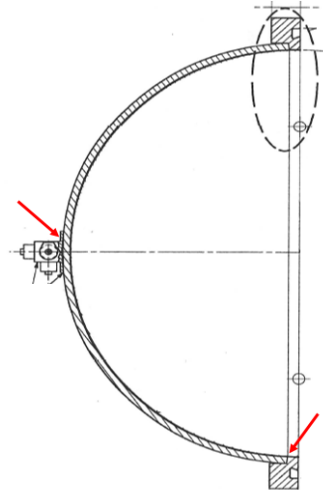


Figure 1: Schematic of hemisphere with flange and accelerometer block. Arrows indicate where welds need to be made.

4.0 Procedure

4.1 Process Selection

To determine the best welding process and post-weld heat treatment (PWHT) a small study was conducted. This study focused on three different welding processes and three types of PWHTs.

4.1.1 Welding

To determine which welding process would be best for this project, three types of welding processes were explored:

- Autogenous electron beam welding (EBW)
- Autogenous gas tungsten arc welding (GTAW)
- Homogenous gas tungsten arc welding (GTAW)

Electron beam welding produces deep penetration welds with minimal heat input, thus minimizing distortion. However, this would need to be produced on the ProBeam which is often booked. Gas tungsten arc welding was pursued because this process produces lower heat input in comparison to other arc welding processes and is always available. Autogenous (no filler) and homogenous (with filler of the same composition as the base material) welding was considered to determine if extra reinforcement from a homogenous weld would be best.

Bead-on-plate welds were made on 17-7PH stainless steel coupons, heat treated to the T-condition. Electron beam welds were performed using the ProBeam and GTA welds

were performed using the Lincoln Electric Precision TIG 375 following the parameters listed in Table 2.

Table 2: Weld parameters for EBW and GTAW welds.

EBW: Autogenous		GTAW: Autogenous		GTAW: Homogenous	
Voltage (kV):	130	Voltage (V):	12.3 – 12.9	Voltage (V):	12.3 – 12.9
Current (mA):	20	Current (A):	120	Current (A):	120
Focus (mA):	TS + 20	Polarity:	DCEN	Polarity:	DCEN
Travel Speed (mm/s):	25.4	Travel Speed (mm/s):	2.9	Travel Speed (mm/s):	2.9
Work Distance (mm):	355.6	Work Distance (mm):	2.4	Work Distance (mm):	2.4
Figure Pattern:	2	Work Angle (°):	90	Work Angle (°):	90
Amplitude X (mm):	0.75	Travel Angle (°):	20	Travel Angle (°):	20
Amplitude Y (mm):	0.75	Direction of Travel:	Leading	Direction of Travel:	Leading
Frequency (Hz):	1000	Wire Feed (mm/s):	N/A	Wire Feed (mm/s):	N/A
Calibration (mA):	5464	Shielding Gas (CFH):	15 UHP Ar	Shielding Gas (CFH):	15 UHP Ar
		Electrode:	1.6 mm dia. 1.5% La	Electrode:	1.6 mm dia. 1.5% La

4.1.2 Post Weld Heat Treatment

The three welded coupons plus a base material coupon were cross-sectioned into three pieces to determine the optimal heat treatment schedule. The different heat treatments used in this study are as follows:

- As-welded (W)
- Welded and aged (W + A)
- Welded, mill anneal, austenite conditioning, and aged (W + 3A)

Heat treatments were performed in the Brew vacuum furnace with an inert gas quench. The as-welded condition specimen were expected to result in the “worst case” for weld strength. Thus, if as-welded samples exhibit a weld strength 50% of the base material, the weld requirements have been met. Subsequent heat treatments were expected to improve the weld strength. Since samples were welded in the T-condition, the PWHT followed the aging heat treatment as this follows the T-condition heat treatment. Since this operation is performed in a vacuum furnace, heat treatment will only take one day, which is preferred for scheduling purposes. To ensure full recovery in hardness of the weld, W + 3A was considered. The heat treatment parameters are shown in Table 3 and the vacuum furnace heat treatment cycles are shown in Appendix A.

Table 3: Heat treatment parameters for the mill anneal, austenite conditioning, and aging steps.

Parameter	Mill Anneal	Austenite Conditioning	Aging
Heating Rate ($^{\circ}\text{C}\cdot\text{min}^{-1}$)	10	10	10
Hold Temperature ($^{\circ}\text{C}$)	1066	760	566
Hold Time (min)	60	90	90
Cooling Rate ($^{\circ}\text{C}\cdot\text{min}^{-1}$)	22.6	8	8.6

4.1.3 Microhardness and Strength

Microhardness maps were collected on the base material and on the welded samples using Struer's Emco Test Durascan hardness indenter with a 500 kgf load. Between 300 and 600 measurements were made per sample. The microhardness was converted to yield strength (YS) and ultimate tensile strength (UTS) following the methodology outlined by Pavlina and Van Tyne [1]:

$$\text{YS (MPa)} = -90.7 + 2.876 \cdot H_v \quad \text{Eq. 1}$$

$$\text{UTS (MPa)} = -99.8 + 3.734 \cdot H_v \quad \text{Eq. 2}$$

The calculated YS and UTS provide an estimate of the actual YS and UTS of the welds, HAZ, and base material. The results of the microhardness and calculated YS and UTS help to determine the PWHT to use for the final components.

4.2 Weld Development: Flange

The plan for welding the flange to the hemi was for the weld to be made on the inside surface. Therefore, for a successful weld, the penetration depth must be equal to or greater than the thickness of the hemi. The thickness of the hemi is expected to range between 4.3 to 4.8 mm (0.17 to 0.19 in); therefore, the depth of penetration should range between 4.4 to 5.0 mm in order to consume the joint.

4.2.1 Parameter Down Select

Bead-on-plate welds were made on 17-7PH stainless steel plate. Welds were then cross-sectioned and characterized to determine the optimal parameters for the joint design. Weld parameters are shown in Table 4 and Table 5. Sharp focus (S) was found using electron optical imaging (ELO) and true sharp focus (TS) was found using the tungsten block method. The welds were then cross-sectioned and characterized to determine which welds met the requirements for the flange and hemi.

Table 4: First set of weld development parameters for bead-on-plate welds.

Parameters	Weld 1.1	Weld 1.2	Weld 1.3	Weld 1.4	Weld 1.5	Weld 1.6
Voltage (kV):	130	130	130	130	130	130
Beam Current (mA):	15	14	13	12	16	17
Weld Focus:	S + 50	S + 50	S + 50	S + 50	S + 50	S + 50
Travel Speed (mm/s):	25.4	25.4	25.4	25.4	25.4	25.4
Work Distance (mm):	610	610	610	610	610	610
Figure Pattern:	6	6	6	6	6	6
Amplitude X (mm):	0.5	0.5	0.25	0.25	0.25	0.25
Amplitude Y (mm):	0.5	0.5	0.25	0.25	0.25	0.25
Frequency (Hz):	800	800	800	800	800	800
Calibration (mA):	7300	7300	7300	7300	7300	7300

Table 5: Second set of weld development parameters for bead-on-plate welds.

Parameters	Weld 2.1	Weld 2.2	Weld 2.3	Weld 2.4
Voltage (kV):	130	130	130	130
Beam Current (mA):	15	14	13	12
Weld Focus:	TS	TS	TS	TS
Travel Speed (mm/s):	25.4	25.4	25.4	25.4
Work Distance (mm):	610	610	610	610
Figure Pattern:	6	6	6	6
Amplitude X (mm):	0.5	0.5	0.5	0.5
Amplitude Y (mm):	0.5	0.5	0.5	0.5
Frequency (Hz):	800	800	800	800
Calibration (mA):	7300	7300	7300	7300

4.2.2 Welding Test Pieces

Electron beam welding was selected as the best process to use. The easiest way to ensure a hermetic seal was to weld on the inside of the hemi. Welding the outside of the hemi would have been difficult due to the curvature of the hemi at the flange (the gap between the hemi and flange would be variable). To gain access to the joint, the component was tilted 7° , therefore a 7° angle will be applied to the joint. Test pieces of simplified geometry were machined out of 17-7PH plate with the angled joint, shown in Figure 2.

The purpose of this experiment is to establish the weld parameters that would be used on the real components, ensure that the weld procedure is repeatable, finalize fabrication steps, and measure distortion from the fabrication process. The fabrication schedule for the test rings is shown in Figure 3. The Romer Arm was used to track the distortion after each fabrication step (machining, heat treatment to the T-condition, welding, and PWHT). After fabrication and measuring the distortion, the test pieces were cross-sectioned for metallography to ensure the weld quality.

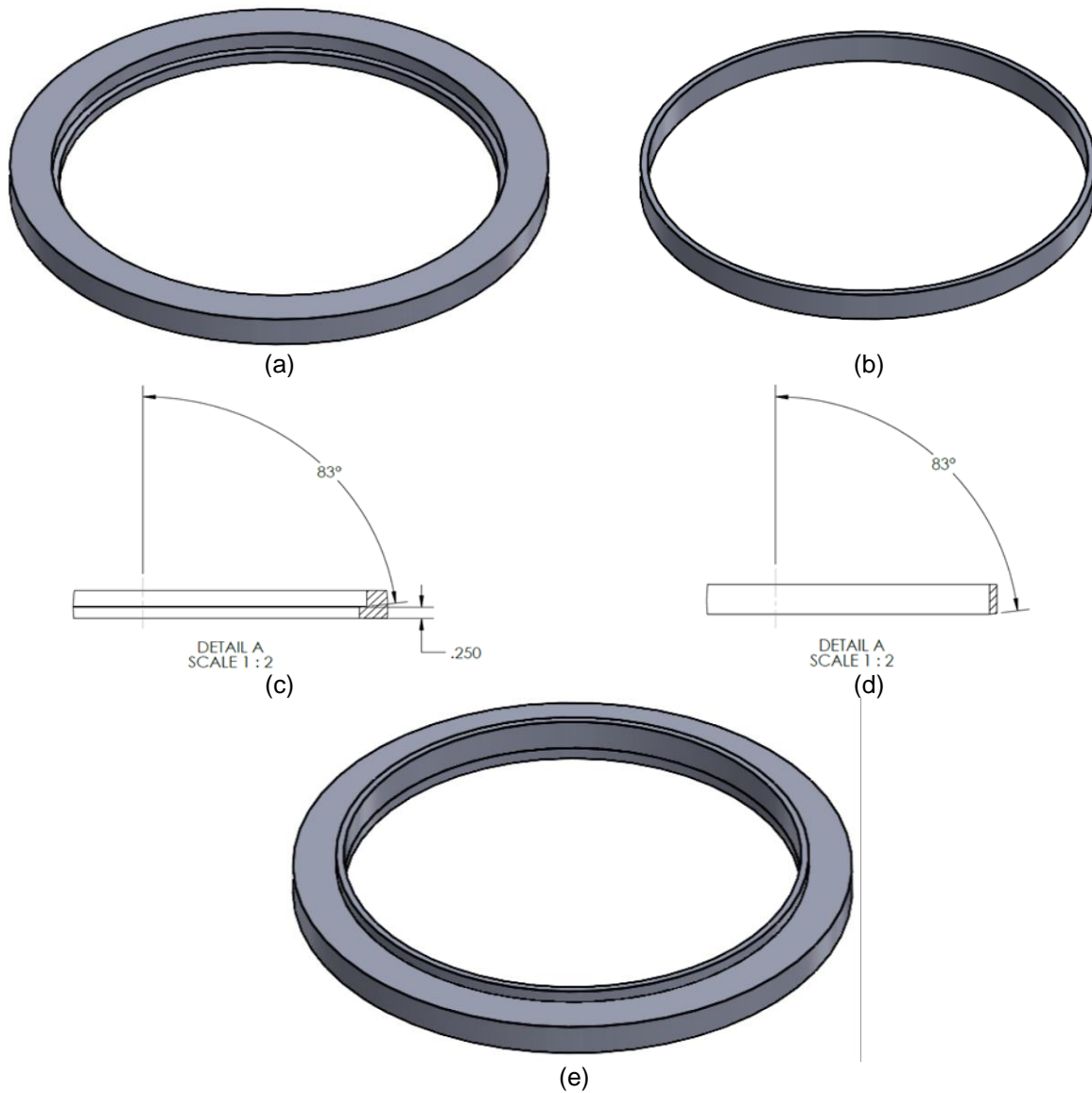


Figure 2: Drawing of the test pieces demonstrating the (a) flange, (b) hemi, (c) angle of the step joint in the flange, (d) angle of the joint in the hemi, and (e) the assembly of the flange and hemi.

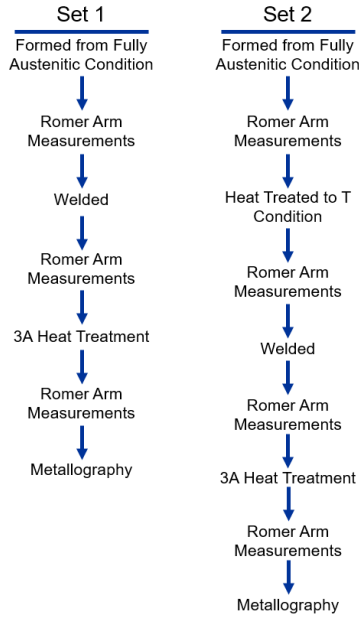


Figure 3: Fabrication schedule for mock test pieces.

4.3 Weld Development: Accelerometer Blocks

The accelerometer block must be attached to the pole of the hemi. The plan was to weld on the outer surface of the hemi to attach the accelerometer. A fillet weld was used for welding this component. The idea behind using a fillet weld is that the majority of the heat is theoretically focused on the flange of the accelerometer block and less onto the main body of the hemi.

4.3.1 Parameter Down Select

Bead-on-plate welds were made on 17-7PH stainless steel plate, heat treated to the T-condition. The parameters used in this study are shown in Table 6. The fillet was then measured using a fillet gauge.

Table 6: Parameter development for accelerator block welds. True sharp focus was found using the tungsten block.

Parameters	Weld 3.1	Weld 3.2	Weld 3.3	Weld 3.4	Weld 3.5	Weld 3.6
Voltage (kV):	130	130	130	130	130	130
Beam Current (mA):	8.5	5.5	3.5	3.5	3.5	3.5
Weld Focus:	S	S	S	S	S	S
Travel Speed (mm/s):	25.4	25.4	25.4	25.4	25.4	25.4
Z Height (mm):						610
Figure Pattern:	17	17	17	0	0	17
Amplitude X (mm):	0.5	0.5	0.25	-	-	0.25
Amplitude Y (mm):	0.5	0.5	0.25	-	-	0.25
Frequency (Hz):	800	800	800	-	-	1000
Calibration (mA):	7300	7300	7300	7300	5172	7800
Tilt (°):	-14	-14	-14	-14	-35	-14

4.3.2 Welding Test Pieces

Partial hemis were formed from 17-7PH blanks, as shown in the schematic in Figure 4. A 0.005 in counterbore was machined into the pole to ensure that the accelerometer blocks were indicated in the correct position. The accelerometer blocks were tacked onto the hemi following parameters from Table 7. Once tacked, the blocks were welded following the parameters in Table 6.

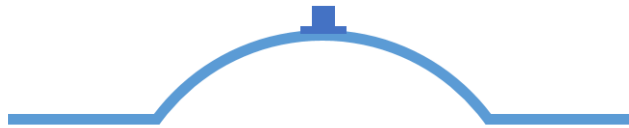


Figure 4: Schematic of a partially formed hemi with the accelerometer block placed on the pole.

Table 7: Tacking parameters for the accelerometer blocks.

Parameters	Weld 2.1
Voltage (kV):	130
Beam Current (mA):	3
Weld Focus:	S
Figure Pattern:	2
Frequency (Hz):	11
Calibration (mA):	7300

4.4 Welding Final Components

5.0 Results and Discussion

This section includes the studies conducted for weld development and the reasoning behind parameters selected.




5.1 Process Selection

This section discusses the reasoning behind the welding process and PWHT that was applied to the final component.

5.1.1 Welding Processes

The three welding processes selected for this study were: autogenous EBW, autogenous GTAW, and homogenous GTAW. A summary of the weld results are shown in Table 8. One of the weld requirements for this study was a minimum penetration depth of 4.3 mm in order to consume the joint. Autogenous EBW can easily achieve this goal with slight adjustments to the parameters, a narrow and deep weld will meet this requirement. Due to the nature of GTAW, the joint design and/or weld parameters would need change in order to meet the weld requirement. Also, due to the minimum distortion requirement, it is well known that GTAW exhibits larger heat inputs in comparison to EBW. Therefore, due to the depth of penetration requirement and minimum distortion requirement, EBW is the welding process that will be used for the final components.

Table 8: summary of the welds performed for the process selection study.

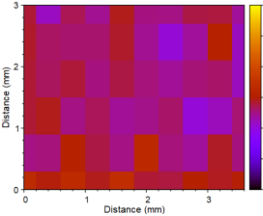
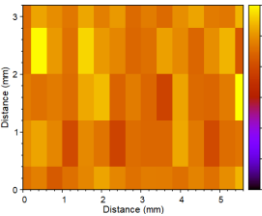
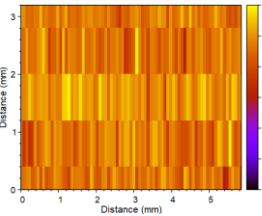
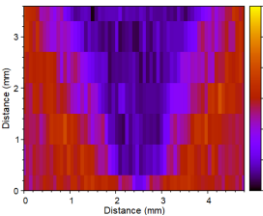
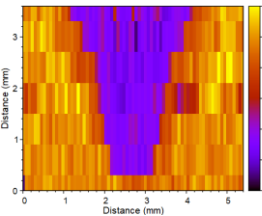
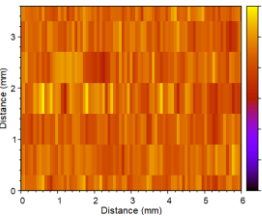
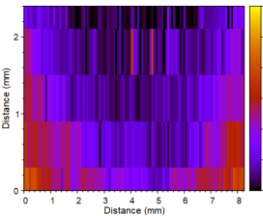
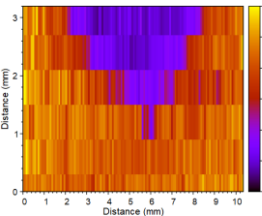
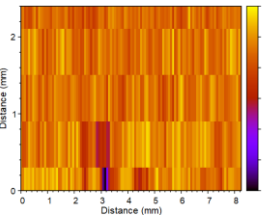
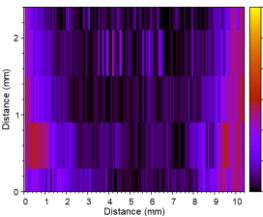
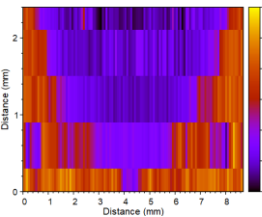
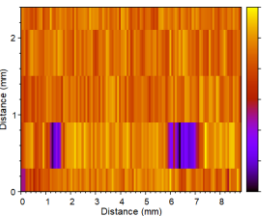
Weld	Depth (mm)	Width (mm)	Macrograph
EBW: Autogenous	3.91	2.66	
GTAW: Autogenous	0.78	5.14	
GTAW: Homogenous	1.12	7.17	

5.1.2 Post Weld Heat Treatment

5.1.2.1 Microhardness

Microhardness maps and average hardness values for the base material, weld metal, and HAZ are summarized in Table 9. Microhardness values of the weld and HAZ were above 50% of the base material for all welding processes and heat treatment conditions, shown in Figure 5. The as-welded condition (W) resulted in the lowest microhardness values, which were about 55% to 64% of the base material. Following the 3A heat treatment (mill anneal, austenite conditioning, and aging) resulted in almost fully recovery of the microhardness (96% to 99% of the base material). Therefore, following welding, a 3A PWHT will be used for the final assembly.

Table 9: Microhardness maps and average microhardness values for the base material, weld metal, and HAZ.

Weld Process	W	W + A	W + 3A
17-7PH Base Material	 Base: 333 ± 15 HV	 Base: 438 ± 21 HV	 Base: 434 ± 23 HV
EBW: Autogenous	 Weld: 233 ± 12 HV HAZ: 295 ± 35 HV	 Weld: 280 ± 21 HV HAZ: 297 ± 31 HV	 Weld: 418 ± 20 HV HAZ: 420 ± 22 HV
GTAW: Autogenous	 Weld: 216 ± 25 HV HAZ: 261 ± 37 HV	 Weld : 248 ± 12 HV HAZ: 273 ± 28 HV	 Weld: 418 ± 20 HV HAZ: 428 ± 30 HV
GTAW: Homogenous	 Weld: 214 ± 22 HV HAZ: 246 ± 41 HV	 Weld: 243 ± 25 HV HAZ: 271 ± 34 HV	 Weld: 428 ± 19 HV HAZ: 420 ± 39 HV

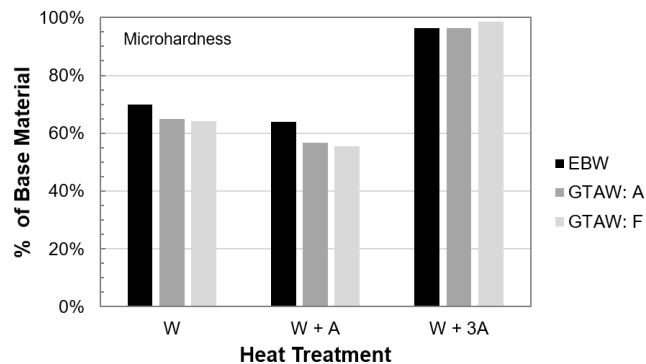


Figure 5: Weld microhardness percent of the base material microhardness.

5.1.2.2 Strength

To better understand if the strength of the weld metal is at least 50% of the base material, YS and UTS maps were plotted (Table 10 and Table 11, respectively). Note that the scale presented for the YS and UTS are the same. The calculated YS and UTS of the weld and HAZ was also above 50% of the base material for all welded processes. These results confirm that the weld meets the requirements. Following the full 3A heat treatment, the average YS and UTS of the weld metal ranged between 96% and 99% of the base material, shown in Figure 6. Thus, confirming that the W + 3A procedure is the best practice and the final components will follow the 3A PWHT schedule.

Table 10: Yield strength maps and average yield strength values of the base, weld metal, and HAZ.

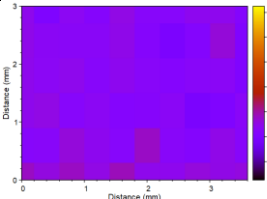
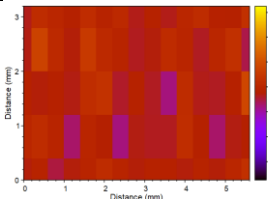
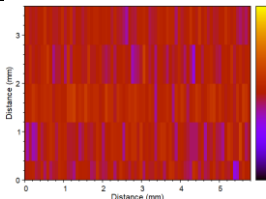
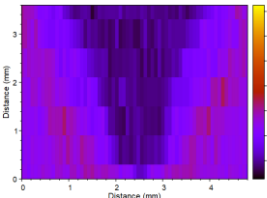
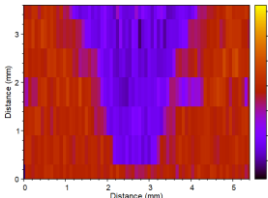
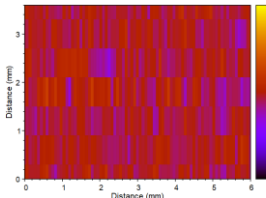
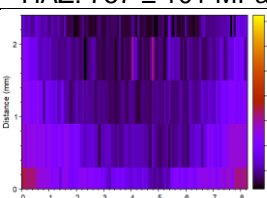
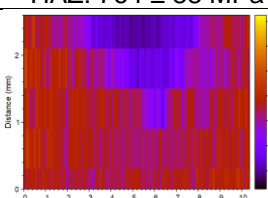
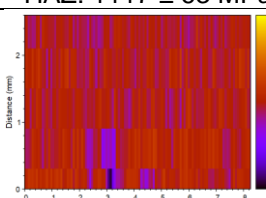
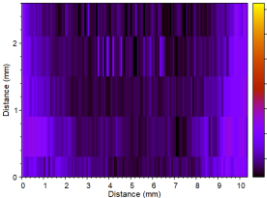
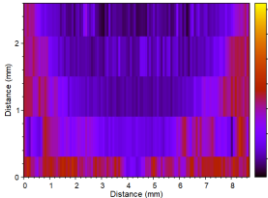
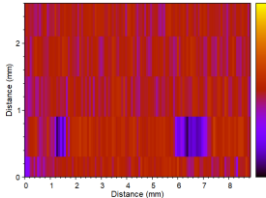
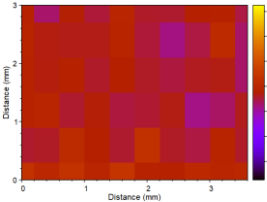
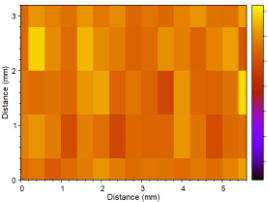
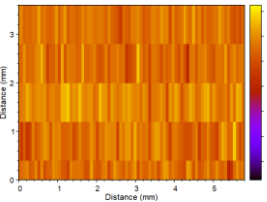
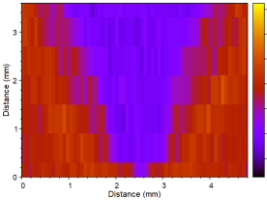
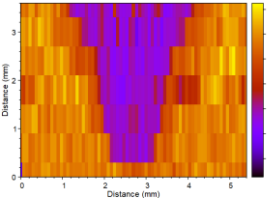
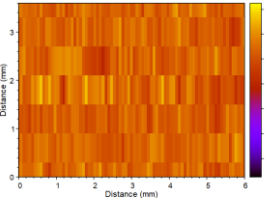
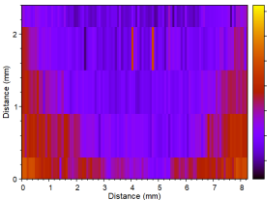
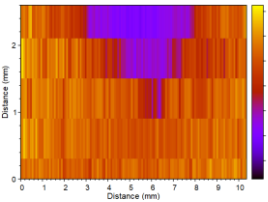
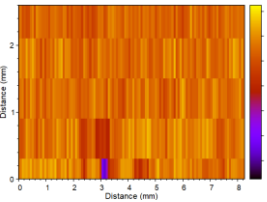
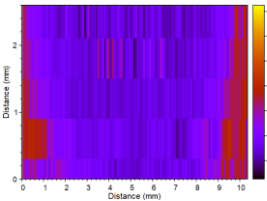
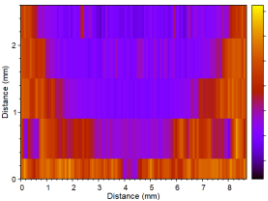
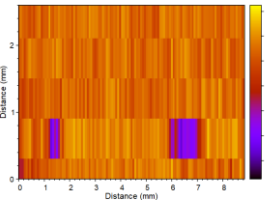
Weld Process	W	W + A	W + 3A
17-7PH Base Material	 Base: 866 ± 42 MPa	 Base: 1170 ± 60 MPa	 Base: 1156 ± 67 MPa
EBW: Autogenous	 Weld: 579 ± 35 MPa HAZ: 757 ± 101 MPa	 Weld: 715 ± 61 MPa HAZ: 764 ± 88 MPa	 Weld: 1113 ± 52 MPa HAZ: 1117 ± 63 MPa
GTAW: Autogenous	 Weld: 530 ± 72 MPa HAZ: 660 ± 105 MPa	 Weld : 825 ± 34 MPa HAZ: 695 ± 124 MPa	 Weld: 1110 ± 55 MPa HAZ: 1142 ± 87 MPa
GTAW: Homogenous	 Weld: 524 ± 64 MPa HAZ: 616 ± 118 MPa	 Weld: 609 ± 71 MPa HAZ: 688 ± 98 MPa	 Weld: 1142 ± 56 MPa HAZ: 1118 ± 112 HV

Table 11: Ultimate tensile strength (UTS) maps and average UTS values of the base material, weld metal, and HAZ.

Weld Process	W	W + A	W + 3A
17-7PH Base Material	 Base: 1143 ± 55 MPa	 Base: 1537 ± 78 MPa	 Base: 1519 ± 87 MPa
EBW: Autogenous	 Weld: 769 ± 45 MPa HAZ: 1000 ± 130 MPa	 Weld: 946 ± 79 MPa HAZ: 1010 ± 115 MPa	 Weld: 1463 ± 68 MPa HAZ: 1468 ± 82 MPa
GTAW: Autogenous	 Weld: 706 ± 93 MPa HAZ: 876 ± 137 MPa	 Weld: 1089 ± 45 MPa HAZ: 920 ± 103 MPa	 Weld: 1459 ± 72 MPa HAZ: 1501 ± 113 MPa
GTAW: Homogenous	 Weld: 699 ± 83 MPa HAZ: 818 ± 153 MPa	 Weld: 807 ± 92 MPa HAZ: 911 ± 128 MPa	 Weld: 1500 ± 72 MPa HAZ: 1470 ± 146 HV

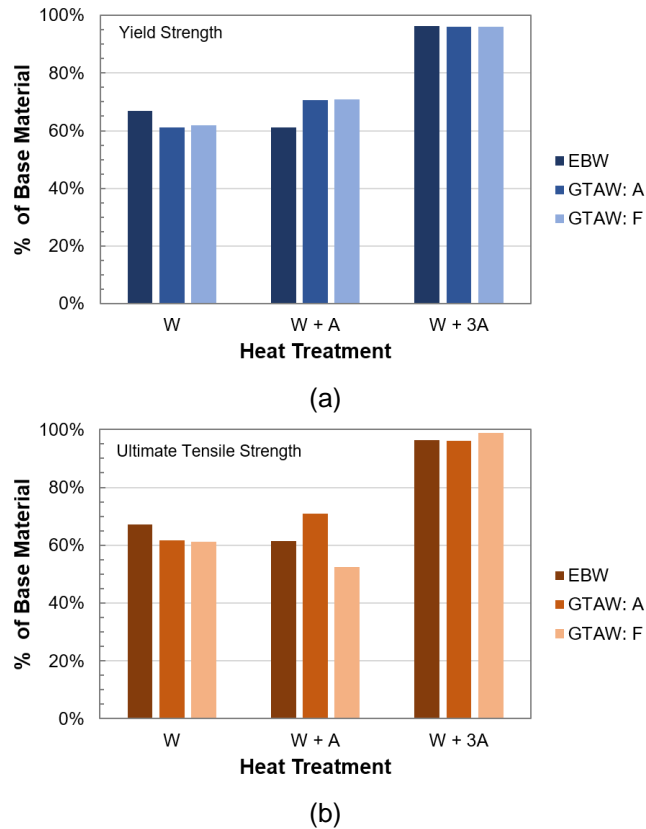




Figure 6: Weld strength as a percent of the base material for (a) yield strength and (b) ultimate tensile strength.

5.2 Weld Development: Flange

5.2.1 Parameter Down Selection

The flange weld needs to consume the joint and create a hermetic seal. This means that the root of the keyhole needs to be relatively wide so as not to miss the joint. A summary of all the welds produced for the parameter down selection can be found in Appendix B. A defocused beam (welds 1.1 through 1.6) resulted in wide, shallow welds which were insufficient for welding the flange. A sharp focus beam (welds 2.1 through 2.4) produced narrow, deep welds which were more sufficient for welding the flange. A beam current of 14 mA and 15 mA produce a penetration depth greater than 4.4 mm (0.17 in), as shown in Table 12. Therefore, the parameters used for welds 2.1 and 2.2 will be used for welding the test pieces.

Table 12: Weld morphology of bead on plate welds selected for the flange weld.

Weld	Depth (mm)	Width (mm)	FWHM (mm)	Micrograph
2.1	4.803	1.261	0.817	
2.2	4.419	1.462	0.761	

5.2.2 Welding Test Pieces

5.2.2.1 Weld Results

An example of a welded test piece is shown in Figure 7. Using a beam current of 14 mA was enough to seal the flange with a hemi thickness of about 3.8 mm as shown by the macrograph in Figure 7. Since this weld was able to consume the entire joint, it is assumed that this would form a hermetic seal. To accommodate a thicker hemi, a beam current of 15 mA was used for the second test piece.



Figure 7: Image of first welded and heat treated test piece using a 14 mA beam current.

5.2.2.2 Distortion Results

Romer arm measurements were taken after each fabrication step: machining, welding, and heat treating. The Romer Arm results of the first test piece are shown in Figure 8. After welding, Figure 7(a), there is a small amount of distortion that ranges between

0.005 in and 0.010 in located in two areas along the flange (designated by the green color). Heat treating the test piece after welding has a larger impact on distortion than the welding operation. The distortion that ranges been 0.005 in and 0.010 in (in green) has grown and these regions are opposite each other (like a potato chip). There is a larger degree of distortion on the outer edge of the flange that ranges somewhere between 0.020 in and 0.025 in. This degree of distortion was expected due to the volume expansion from the martensitic phase transformation and is unavoidable. Overall, it was decided that this amount of distortion should not affect the seal between the flanges.

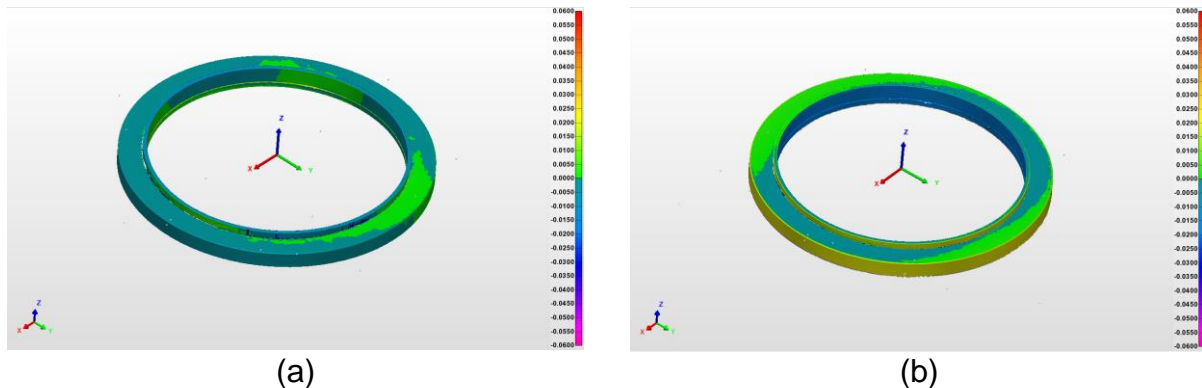


Figure 8: Romer arm results of the first test piece after (a) welding and (b) 3A heat treatment.

5.3 Weld Development: Accelerometer Blocks

5.3.1 Parameter Down Selection and Welding Test Pieces

The results of the welded accelerometer blocks are shown in Figure 9. The initial parameters selected for this weld (Weld 3.1) were too large with a resulting fillet of about 0.125 in. The beam current was too large for this weld, but also, the calibration used for this weld was not the correct calibration and therefore the figure pattern amplitudes were most likely larger than expected. Lowering the beam current was helpful in reducing the size of the fillet. Weld 3.2, Figure 9(b), was also considered too big and Weld 3.5, Figure 9(e), was considered to be too small and potentially unreliable. The best fillets were Weld 3.3 and 3.6, Figure 9(c) and (f), with a fillet size of 3/32.

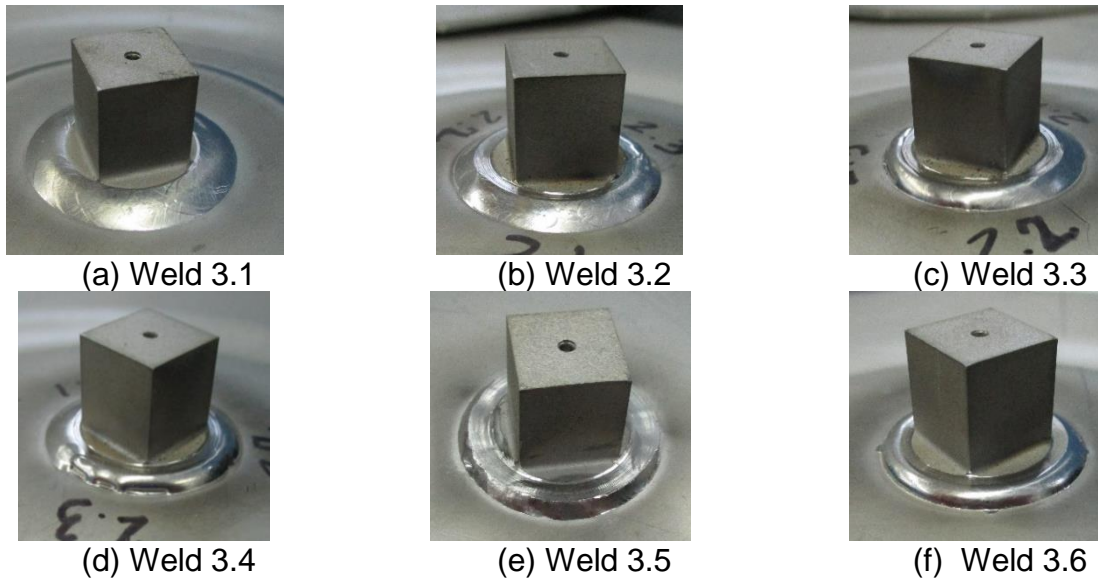
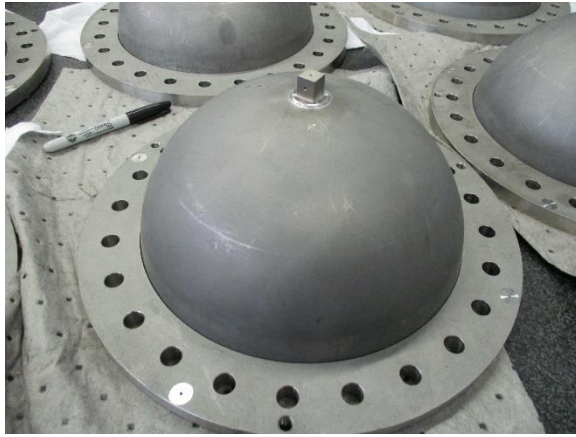


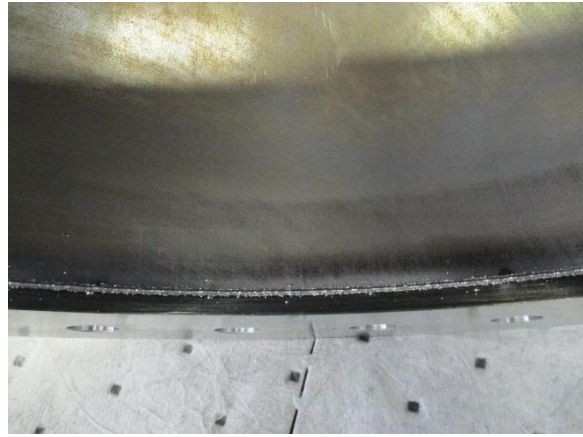
Figure 9: Accelerometer block welds made under different weld parameters with a resulting fillet size of (a) 1/8 in, (b) , (c) 9/64 in, (d) 3/32 in, (e) 5/64 in, and (f) 3/32 in.

5.4 Welding Final Components

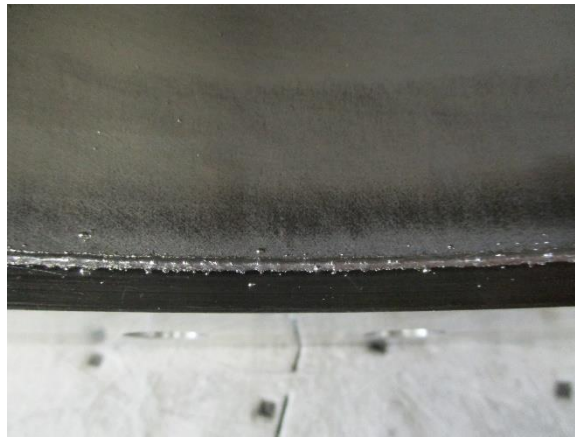
The final welded assembly is shown in Figure 10. The hemis were welded with the final parameters shown in Table 13. The flange and hemi were tacked using GTAW to ensure that there was no misalignment when fixturing the component to the ProBeam table. There were slight fit-up differences between the test pieces and the real components. The real components had more spatter than the test pieces. In addition, short sections where there was poor fit up contained concave reinforcement. These concave regions would most likely have been machined away, but since this is undesirable, we manually filled in the concave sections using GTAW.



(a)



(b)



(c)

Figure 10: Image of the final welded hemi assembly demonstrating the (a) outer surface and accelerometer block weld, (b-c) the inner surface flange weld.

Table 13: Final weld parameters used to weld the flange and accelerometer blocks to the hemis.

Parameters	Flange	Tack	Accelerometer Block
Voltage (kV):	130	130	130
Beam Current (mA):	15	3	3.5
Weld Focus:	TS	S	S
Travel Speed (mm/s):	25.4		25.4
Figure Pattern:	6	2	17
Amplitude X (mm):	0.5		0.25
Amplitude Y (mm):	0.5		0.25
Frequency (Hz):	800	11	1000
Calibration (mA):	7300		
Tilt (°):	-83° (7°)	-14°	-14°
Inslope:	10°	--	10°
Outslope:	20°	--	10°
Vector:	--	--	270°

6.0 Conclusion

A welding procedure and post weld heat treatment was successfully developed to limit the amount of distortion to the flanges and best match the weld hardness with the parent material hardness.

7.0 References

- [1] E. J. Pavlina and C. J. Van Tyne, "Correlation of Yield Strength and Tensile Strength with Hardness for Steels," *Journal of Materials Engineering and Performance*, vol. 17, no. 6, pp. 888 – 893, Dec. 2008. doi: 10.1007/s11665-008-9225-5

8.0 Appendices

8.1 Appendix A – Heat Treatment Schedules

Table A.1: Vacuum furnace program for the mill anneal, austenite condition, and aging heat treatments.

Cycle	Mill Anneal		Austenite Conditioning		Aging	
	Temp (°C)	Time (min)	Temp (°C)	Time (min)	Temp (°C)	Time (min)
R	0	110	0	76	0	57
R	1066	1	760	1	566	1
S	1066	1	760	1	566	1
R	1066	2	760	2	566	2
S	1066	60	760	90	566	90
R	1066	45	760	90	566	60
S	50	2	50	2	50	2
	He cool		Ar cool		Ar cool	

8.2 Appendix B – Bead-on-Plate Welds

This section contains a summary of the results from weld development for the flange weld and accelerometer block weld.

Table B.1: Summary of the weld morphology for flange welds produced with a defocused beam including the depth of penetration, width (measured from toe-to-toe), full width half max, and macrograph.




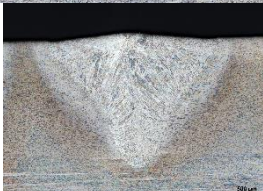


Weld	Depth (mm)	Width (mm)	FWHM (mm)	Micrograph
1.1	3.027	3.327	1.332	
1.2	2.709	3.213	1.356	
1.3	2.032	2.833	1.413	
1.4	2.152	2.881	1.383	
1.5	2.222	2.957	1.409	
1.6	2.311	2.961	1.487	

Table B.2: Summary of the weld morphology for flange welds produced with a sharp focused beam including the depth of penetration, width (measured from toe-to-toe), full width half max, and macrograph.





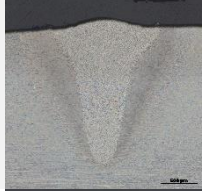
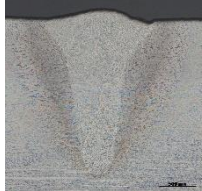


Weld	Depth (mm)	Width (mm)	FWHM (mm)	Micrograph
2.1	4.803	1.261	0.817	
2.2	4.419	1.462	0.761	
2.3	4.122	1.401	0.807	
2.4	4.106	1.646	0.763	

Table B.3: Summary of the weld morphology for the accelerometer block welds produced with a sharp focused beam including the depth of penetration, width (measured from toe-to-toe), full width half max, and macrograph.

Weld	Depth (mm)	Width (mm)	FWHM (mm)	Micrograph
3.1	1.908	1.522	0.635	
3.2	2.142	1.536	0.641	
3.3	2.310	1.582	0.719	
3.4	2.537	1.624	0.691	
3.5	2.809	1.608	0.681	